Geometry of Renormalization Group Flows Constrained by Discrete Global Symmetries

C.A. Lütken*

Department of Physics, University of Oxford
1 Keble Road, Oxford OX1 3NP, United Kingdom

August 1992

Abstract

The connection between the phase structure and the geometry of the renormalization group (RG) flow in systems with discrete *parameter space* symmetries is studied. These are symmetries of the partition function, and therefore determine the geometry of the phase diagram for the system. The C-function, which is the potential for the RG flow, inherits the symmetries of the partition function, so that the RG flow must respect the geometry of the phase diagram. It is suggested that if the symmetry group is sufficiently large, i.e. an infinite discrete non-abelian group, then it may constrain the C-function so much that global (topological) information about the RG can be obtained. A systematic taxonomy of possible phase and flow diagrams associated with subgroups of the modular group at level two is given, and applications to the quantum Hall effect and high-temperature superconductivity are discussed.

*Address after 1.10.92: NORDITA, Blegdamsvej 17, DK-2100 Copenhagen Ø, Denmark

1 Introduction

Partition functions may be invariant under two different types of transformations: symmetries of the action (or Hamiltonian) and symmetries of the parameter space. We are perhaps most familiar with the former, which include space-time invariances as well as gauge symmetries. It is the purpose of this letter to focus on the latter and show how such symmetries can be used to elicit global information about the phase diagram and renormalization group (RG) flow of the system.

The motivation for these considerations come from an attempt [1] to understand the "macroscopic" properties of the subtle and resilient quantum Hall system. The main result is a new phase and RG-flow diagram for this system, which unlike the one proposed earlier [1] can only be valid in the strong magnetic field limit, where even denominator plateaus are forbidden. In spite of the great superficial difference between these diagrams, they are intimately related. This will be formally evident from the group-theoretical considerations below, but can also be seen in a more direct geometrical and analytical way by studying RG-potentials. These functions provide a simple conceptual framework wherein entire (infinite) classes of phases can be switched on or off by tuning external control parameters. The global phase and flow diagrams presented here encode various aspects of electron transport in an external magnetic field in two dimensions, and may account for all the peculiar universality properties which have been observed in this system.

Some of the ideas to be discussed here originated in an effort to understand non-perturbative properties of certain quantum field theories of interest in high-energy physics [2, 3], but have recently resurfaced in the context of charge transport in two dimensions [4, 1]. It would appear that the field theories of interest in condensed matter physics exhibit many novel features which are usually not needed in high-energy physics. This is partly due to the fact that it is easy to manufacture samples whose effective dimension is less than three. Because we in two dimensions or less are no longer restricted to consider just fermions or bosons, low-dimensional systems may exhibit a plethora of ground states whose excitations (quasi-particles) can carry exotic spin, charge and statistics (anyons)

[5].

Two exciting experimental discoveries during the eighties have catapulted these ideas to the frontline of theoretical physics: both the quantum Hall effect and high-temperature superconductivity are believed to be consequences of the materials being effectively two-dimensional as far as charge transport is concerned. While it is clearly an important problem to understand how such "anomalous" transport emerges as a macroscopic property of (2+1)-dimensional quantum electrodynamics in disordered media, we shall here instead pursue a much simpler *phenomenological* approach proposed in Ref. [1].

Transport coefficients or response functions are macroscopic quantities appearing in the effective action, which encodes only the low energy properties of the system. At large scales they parametrize the space on which the renormalization group acts, and it is the phase and fixed point structure of this parameter (conductivity or resistivity) space which is explored when resistances are measured. Since these are global properties of the effective field theory, it would appear that a theoretical determination of these data is a hopeless non-perturbative task. However, in Ref. [1] a way around this impasse was suggested. The main idea is that an infinite global discrete parameter space symmetry, analogous to the Kramers-Wannier (KW) duality exhibited by most spin systems, may be sufficient for determining the geometry of the phase and RG-flow diagram, including the exact location of all renormalization group fixed points. This reduces our task to determining the global symmetries of the partition function. Using only the most rudimentary experimental data as input, it is surprisingly easy to make a "phenomenological ansatz" for the form of this symmetry. It appears to be very difficult to *prove* that such a symmetry follows from the microphysics [6], but because it leads to a wealth of experimentally accessible predictions such an ansatz is far from vacuous. Indeed, not only does it correlate all scaling data and suggest new experiments, because the symmetries we have in mind are not easily satisfied they should also be very useful for pinning down the correct effective quantum field theory [6].

In the next section the basic idea is explained by reference to the simplest example, which is the Ising model. In this case KW-duality is a rather trivial $\mathbb{Z}_2$

symmetry, but this is still sufficient to illustrate the interplay between the phase and RG-flow structure of the parameter space.

Sect. 3 discusses the generalization to two-dimensional flows constrained by infinite discrete non-abelian groups, in particular the modular group and its subgroups at level two. Most of the group theoretical facts needed in our discussion have been collected in this section.

In Sect. 4 the phase and flow diagrams associated with subgroups of the modular group at level two are constructed using functions automorphic under the groups, since these functions mimic the RG potentials or "C-functions" which must respect the discrete global symmetries of the partition function.

In Sect. 5 possible applications of these ideas to "anomalous" charge transport phenomena in two dimensions, namely the quantum Hall effect and high-temperature superconductivity are discussed. This leads to an infinite number of predictions which in principle can be checked experimentally. A brief account of some of these ideas was given in Ref. [7].

Some observations, conjectures and philosophical remarks are collected in the final section.

2 The Ising Model

The symmetries with which we will be concerned here are in some sense generalizations of ordinary Kramers-Wannier duality, which already appears in the two-dimensional Ising model [8]. In the isotropic case the only parameter of the Ising model is the temperature ($T = \beta^{-1}$), and KW-duality is the fact that the high-temperature partition function $\mathcal{Z}(\beta)$ is identical to the low-temperature partition function $\mathcal{Z}(\beta')$, where $\beta' = -\frac{1}{2}\log \tanh\beta$. Provided we know or assume that the model has a unique second order phase transition at a finite temperature T_c, this symmetry can be used to determine the exact value of T_c, since it in this case must coincide with the self-dual point where $\beta = \beta' = -\frac{1}{2}\log(\sqrt{2}-1)$.

The geometrical content of KW-duality becomes more transparent after a non-linear reparametrization $\beta \to y = (1+\exp(-2\beta))/\sqrt{2}$, in terms of which the

KW-transformation is realized by a (fractional) linear transformation:

$$y \to y' = \frac{1}{y}. \tag{1}$$

Thus, KW-duality is a global discrete abelian $\mathbb{Z}_2$ symmetry which maps high temperature Ising models onto low temperature Ising models, and *vice versa.*

Having mapped out the global phase diagram using the constraints provided by the discrete KW-symmetry, the next question is what this tells us about the structure of the RG-flow. Since the RG acts on the parameter space, and since RG-flows cannot cross phase boundaries (in the Ising case the boundary is just the point T_c which bisects the parameter space – the real positive line – into the ordered low-temperature and disordered high-temperature phases), it is clear that KW-type symmetries (i.e. discrete global symmetries acting on the parameter space) severely constrains the topology of the RG-flow. It is also clear, however, that a geometrical argument of this type can tell us nothing about the sign or value of the critical exponents, since this requires dynamical information, or, equivalently, information about the RG-flow near the fixed points $T^* = 0, T_c, \infty$.

It is believed that all information about the RG is contained in the so-called *RG-potential*, which is a real valued function of the coupling constants (g_i) of the theory [9]. In two dimensions this is a fact which is incorporated in Zamolodchikov's C-theorem [10], which states that there always exists (in two dimensions) such a function $C(g_i)$ which is monotonically decreasing along the flow generated by rescalings, and whose value at a critical point (g_i^*) is the central charge, $c = C(g_i^*)$, of the conformal field theory describing the massless modes at that fixed point. We can interpret the C-function as measuring the density of effectively massless degrees of freedom at each scale [11]. It is clear that this number must decrease along the flow, since relevant perturbations can only reduce the number of effectively massless modes, so that the C-function must be a "negentropic" information measure on the space of theories under consideration, and this is indeed what the C-theorem asserts. When the RG-flow is such a gradient flow (i.e. the β-functions are the gradients of C) it is impossible to have limit cycles or other pathologies, which must be excluded for physical reasons [9].

In short, the C-theorem leads to a simple and appealing geometrical ("to-

pographical") picture of the RG: fixed points of the RG correspond to critical points of the C-surface over the parameter space ($\ominus \equiv$ repulsive point = mountain top, $\oplus \equiv$ attractive point = valley bottom, $\otimes \equiv$ saddle point = mountain pass), and phase boundaries correspond to ridges separating different valleys. All β-functions automatically vanish at critical points and the anomalous dimensions encode the curvature of the C-surface at the fixed points.

It should now be clear that the RG-flow must respect any global symmetries controlling the phase structure of the system. This connection between the symmetries of the partition function and the symmetries of the C-function can be formalized by exploiting the fact that C is essentially the vacuum or free energy (F) of the system: $C \sim F \sim \log \mathcal{Z}$, at least in the context of finite size scaling [12]. This must be so because the C-function can only be built from operators which couple to all degrees of freedom in the complete family of theories parametrized by g_i. In two dimensions the unique candidate appears to be the stress-energy tensor, and this is indeed the only ingredient needed to construct Zamolodchikov's C-function. C is the crudest possible caricature of $\mathcal{Z}$, recording only the number of effective degrees of freedom at each scale, but it must respect the global discrete KW-like symmetries possessed by $\mathcal{Z}$.

To see how all this works in detail in the simple Ising case, we must choose a specific action for the model. Following Cardy [3] it is convenient to use the massive Majorana fermion representation:

$$S_I = \int d^2\zeta(\psi\bar{\partial}\psi + \bar{\psi}\partial\bar{\psi} + im\bar{\psi}\psi). \tag{2}$$

Completing the calculation started in Ref. [3], we[1] find that the C-function

$$C = 2\langle TT\rangle - \langle \Theta T\rangle - \frac{3}{8}\langle\Theta\Theta\rangle, \tag{3}$$

where the holomorphic (T) and trace (Θ) parts of the stress tensor in this parametrization are $T = -\pi : \psi\partial\psi :$ and $\Theta = 2\pi im : \bar{\psi}\psi :$, is given by

$$2C_I(|m|) = (|m|^2 - |m|^4)K_1^2(|m|) + |m|^4 K_0^2(|m|) + |m|^3 K_0(|m|)K_1(|m|), \tag{4}$$

in terms of the Bessel functions K_0 and K_1. The critical Ising model is obviously described by the massless theory, which is conformal with central charge $c = 1/2$,

[1] I am grateful to J. Latorre for details on this point.

and $C_I(0)$ is indeed $1/2$, as asserted by the C-theorem. $C_I(\infty) = 0$, corresponding to the trivial (attractive) fixed points at zero temperature (completely ordered) and infinite temperature (completely disordered) with no massless degrees of freedom. The Ising C-function is represented in Fig. 1, together with the (one-dimensional) phase and flow diagram it induces. In the following we shall be concerned with generalizations of these ideas to two-parameter flows constrained by infinite non-abelian discrete groups, in particular the modular group $\Gamma(1) \equiv \mathrm{SL}(2,\mathbb{Z})$ and its subgroups at level two. Since we may choose a complexified version of (1):

$$S: \quad z = x + iy \to z' = -\frac{1}{z} \tag{5}$$

as one of the generators of $\Gamma(1)$, we shall sometimes call modular symmetry "complexified KW-duality" in order to remind ourselves of its physical interpretation in this context.

3 Complexified KW-Duality

In this section we collect the relevant group theoretical facts which will be needed in the following. Since the class of symmetries with which we will be concerned here is not much used in physics, outside of string theory, we shall expend some effort in trying to understand how to deal with infinite discrete non-abelian groups. We start by discussing the simplest and in many ways most interesting of these: the modular group $\Gamma(1) \equiv \mathrm{SL}(2,\mathbb{Z})$.

In order to give a physical motivation for the introduction of this unusual group, consider the coupled clock models. Expressed in a somewhat unconventional way, in terms of two multivalued scalar fields ϕ^a $(a = 1,2)$ restricted to take values in the integers mod p ($\mathbb{Z}_p$-valued spins on dual lattices), the coupled clock model action is of the simplest possible form containing no more than two derivatives:

$$\begin{aligned} \mathcal{L}_p^{cc} &= -y\delta_{\mu\nu}\delta_{ab}\partial^\mu\phi^a\partial^\nu\phi^b + ix\epsilon_{\mu\nu}\epsilon_{ab}\partial^\mu\phi^a\partial^\nu\phi^b \quad (y>0) \\ &= 2i(z\partial\varphi\bar{\partial}\bar{\varphi} - \bar{z}\partial\bar{\varphi}\bar{\partial}\varphi). \end{aligned} \tag{6}$$

Here x and y are real parameters, $z = x + iy$ is a complex parameter, and on a lattice $\partial_\mu\phi^a$ means the difference in ϕ^a evaluated at neighbouring points in

the μ'th direction ($\mu = \zeta^1, \zeta^2$). The last equality is obtained by introducing the complex coordinate $\zeta = \zeta^1 + i\zeta^2$ ($\partial = \partial/\partial\zeta$), the complex scalar field $\varphi = \phi^1 + i\phi^2$, and their complex conjugates (denoted by overbars). The neat appearance of the complex parameter z in this action suggests that the moduli space is the complex upper half plane $\mathbb{H} = \{z \in \mathbb{C} | \mathrm{Im}\ z > 0\}$. It is the symmetries of this space which will concern us in the following, but before discussing these we would like to suggest why it may be *natural* to consider coupled clock models in the context of two-dimensional electron transport.

Since spin systems are ubiquitous in theoretical physics as canonical representatives of universality classes, the choice of p-state lattice models requires no further comment. But why must we consider *two* coupled copies?

The reason would appear to be that we are trying to model a system which is frustrated by a competition between Bose-condensation and Pauli-exclusion. Normally this situation does not arise, but since intermediate statistics (anyons) is possible in two dimensions there are many compromises that can be struck beyond the two extreme cases to which we are restricted in higher dimensions. This leads to the rich zoo of cooperative phenomena present in the quantum Hall system. Depending on the values of the external "control" parameters, the system may find it energetically favourable to have the particles condense into a new ground state – e.g. one of the fractional phases appearing in the quantum Hall system. The spectrum of unconfined excitations around this state constitute the new particles, which may subsequently condense, etc.

In short, we need *competition* to achieve the *cooperation* exhibited in this system. The simplest way to encode this in an action seems to be by adding together a symmetric and an anti-symmetric term with *independent* coefficients, as shown in (6). The rôle of the anti-symmetric term is to couple the lattice to the dual lattice.

As first shown by Cardy [3] the partition functions of these models are invariant under modular transformations:

$$\mathcal{Z}_p^{cc}(\gamma(z), \gamma(\bar{z})) = \mathcal{Z}_p^{cc}(z, \bar{z}) = \mathrm{Tr}\ \exp\{-\int d^2\zeta \mathcal{L}_p^{cc}(z, \bar{z})\}, \quad \gamma \in \Gamma(1). \qquad (7)$$

The modular group $\Gamma(1)$ is generated by translations $T(z) = z + 1$ and inver-

sions $S(z) = -1/z$. The rich structure of this group is entirely due to the fact that S and T do not commute. Hence, if we consider only one clock model, so that no anti-symmetric term is possible, then the only remnant of $\Gamma(1)$ is the real transformation $S(y) = 1/y$, which is just the abelian $\mathbb{Z}_2$ Kramers-Wannier transformation (1).

It is well-known that this symmetry can be used to locate critical points of spin models [8]. Since $\mathcal{Z}_p^{cc}(iy)$ reduces to the p-state Potts model in the thermodynamic limit ($p = 2$ is the Ising model), we know [13] that there is a unique second order phase-transition at the self-dual point ($z = i$, $y = 1$) when $p \leq 4$, and that the transition is first order when $p > 4$. This famous result was generalized in Refs. [2, 3] to the coupled clock models. A simple comparison of energy and entropy showed that this phase-boundary extends in a unique way away from $z = i$, provided that $p < 2\sqrt{3}$. The rest of the phase boundary is then uniquely fixed by modular invariance, so that for $p = 2, 3$ (coupled Ising and 3-state Potts models) the phase diagram is given by the "tree" of solid lines shown in Fig. 2. (The flow lines on the tree in Fig. 2 do not correspond to any of Cardy's models.) For higher values of p a new "Coulomb" phase injects itself along this phase boundary, and for large p it grows to dominate the phase diagram.

From the fact that the phases of the diagram in Fig. 2 only touch the real axis at fractional values, it is immediately clear why $\Gamma(1)$ is a promising group for the quantum Hall problem: if z can be identified with the *complexified conductivity* $\sigma = \sigma_{xy} + i\sigma_{xx}$, then σ_{xy} will be forced by the phase-diagram alone to take fractional values when σ_{xx} vanishes. Note that in this effective field theoretical description no distinction is made between integer and fractional phases, and we cannot have one without the other. Furthermore, as shown in Ref. [1], the location of the bifurcation points where new fractional phases become possible as σ_{xx} is reduced, agree remarkably well with available scaling data from the quantum Hall system.

The bifurcation points are obviously fixed points of the renormalization group since RG flows cannot cross phase boundaries. That they are also fixed points of $\Gamma(1)$ follows from the fact that the modular group is the free product of $\mathbb{Z}_2$ (generated by S) and $\mathbb{Z}_3$ (generated by $Q = ST$). This implies that there are two

types of fixed points on the tree, of order two ($S^2 = 1$) and three ($Q^3 = 1$). The bifurcation point at $z = j \equiv \exp(\pi i/3)$ is an "elliptic" fixed point of order three ($\in \mathbb{E}_3$) ($\ominus$ in Fig. 2), because $Q(j) = Q^2(j) = j$. Since modular transformations are conformal angles are preserved under Q and the phase boundaries meeting at j must do so at an angle of $2\pi/3$. For the same reason every image $\gamma(j)$ ($\gamma \in \Gamma(1)$) of j is also a "Mercedes star", i.e. a fixed point of order three. Similarly, $z = i$ is an "elliptic" fixed point of order two ($\in \mathbb{E}_2$) ($\otimes$ in Fig. 2), because $S(i) = i$, and so are all its images $\gamma(i)$. The latter are natural candidates for delocalization fixed points, and this also fits well with scaling data on the transition between many integer levels.

In addition, there are two other types of fixed points not located on the self-dual tree. Strictly speaking, they do not lie in the parameter space $\mathbb{H}$ at all, but on its compactification $\overline{\mathbb{H}} = \mathbb{H} \cup \mathbb{Q} \cup \{i\infty\}$. The rationals $\mathbb{Q}$ are "parabolic" fixed points ($\mathbb{P}$) of $\Gamma(1)$, and have already been identified with the attractive RG fixed points ($\oplus$ in Fig. 2) corresponding to Hall plateaus. The "hyperbolic" fixed point at $i\infty$, which is also an attractor in this case, seems to be associated with some kind of metallic or superconducting phase.

There are three distinct scaling diagrams consistent with this fixed point structure, depending on whether $\gamma(i)$ is a saddle point, a repulsive point, or part of a marginal line of fixed points along the phase boundary. This ambiguity comes about because KW-type symmetries only pin down the critical *values* of parameters, some additional data are required in order to identify the universality class and thus the scaling exponents encoding the rate at which critical points in moduli space are approached. However, based on our experience with RG flows, we expect the additional information needed to be rather limited. Roughly speaking, only a rudimentary knowledge of the degrees of freedom and their symmetries should suffice, and this is the spirit in which we shall approach the quantum Hall problem. If we restrict attention to the class of self-dual ($\Gamma(1)$-invariant) models which interpolate between the coupled clock models, defined by analytic continuation in p to any positive real p, then the only remaining ambiguity is in the value of p.

Let us now turn to the congruence subgroups of $\Gamma(1)$ at level two. These all

lie between $\Gamma(1)$ and $\Gamma(2)$, where

$$\Gamma(N) \equiv \{\gamma \in \mathrm{SL}(2,\mathbb{Z}) | \gamma = I \pmod{N}\} \tag{8}$$

is called the principal congruence group at level N. Obviously $\Gamma(1) = \mathrm{SL}(2,\mathbb{Z})$. A congruence group is a group that contains $\Gamma(N)$ for some finite value of N. At level two there are only four congruence groups in addition to $\Gamma(2)$, which are related to the six cosets in $\Gamma(1)/\Gamma(2)$. The three that interest us are defined by:

$$\Gamma_{\mathrm{R}}(2) \equiv \{\gamma \in \Gamma(1) | \gamma = I, R \pmod{2}\}, \tag{9}$$

where $R = T, S, W$ $(W = TST)$, while the fourth, which conventionally is labeled by $P = ST = S^{-1}QS$, is slightly different:

$$\Gamma_{\mathrm{P}}(2) \equiv \{\gamma \in \Gamma(1) | \gamma = I, P, P^2 \pmod{2}\}. \tag{10}$$

These groups are all generated by two non-commuting generators, which we can choose as follows:

$$\begin{aligned} \Gamma(1) &= \{T, S\}, & \Gamma_{\mathrm{T}}(2) &= \{T, ST^2S\}, & \Gamma_{\mathrm{S}}(2) &= \{S, T^2\}, \\ \Gamma_{\mathrm{W}}(2) &= \{W, T^2\}, & \Gamma_{\mathrm{P}}(2) &= \{P, SPS\}, & \Gamma(2) &= \{T^2, ST^2S\}. \end{aligned} \tag{11}$$

To see what these symmetries have to do with the quantum Hall system, note that we are interested in symmetries which partition the rationals into the various equivalence classes which appear in the quantum Hall experiments. Clearly $\Gamma(1)$ maps any rational number into any other, which is why every rational number labels one of the phases in the $\Gamma(1)$-invariant phase diagram (Fig. 2). There are, however, other ways to tessellate the upper half plane, which is reflected in the way $\Gamma \subset \Gamma(1)$ treats the rationals.

The special significance of the principal congruence group $\Gamma(2)$ is that it respects the parities of the fraction $p/q \in \mathbb{Q}$, i.e. if p is even (odd) then so is its image under $\gamma \in \Gamma(2)$, and similarly for q. Thus $\Gamma(2)$ splits the rationals into three equivalence classes, which, if we let "0" denote "even" and "1" denote "odd", are conveniently labeled by $0/1 = 0, 1/1 = 1$ and $1/0 = \infty$. ($0/0$ is ill-defined, i.e. there is no $0/0$ class because two even numbers are not relatively prime.) The congruence groups $\Gamma_{\mathrm{T}}(2), \Gamma_{\mathrm{S}}(2)$ and $\Gamma_{\mathrm{W}}(2)$, being intermediate between $\Gamma(1)$ and

$\Gamma(2)$, splits the rationals into just two equivalence classes each: because $\Gamma_{\mathrm{T}}(2)$ contains T it maps 0 to 1, because $\Gamma_{\mathrm{S}}(2)$ contains S it maps 0 to ∞, and because $\Gamma_{\mathrm{W}}(2)$ contains W it maps 1 to ∞.

In short, these groups partition the rationals $p/q \in \mathbb{Q}$ as follows:

$$\begin{aligned}
\Gamma(1): &\quad \{0 \sim 1 \sim \infty\} = \mathbb{Q} \\
\Gamma_{\mathrm{T}}(2): &\quad \{0 \sim 1,\ \infty\} = \{q \in 2\mathbb{Z}+1\} \cup \{q \in 2\mathbb{Z}\} \\
\Gamma_{\mathrm{S}}(2): &\quad \{0 \sim \infty,\ 1\} = \{pq \in 2\mathbb{Z}\} \cup \{pq \in 2\mathbb{Z}+1\} \\
\Gamma_{\mathrm{W}}(2): &\quad \{0,\ 1 \sim \infty\} = \{p \in 2\mathbb{Z}\} \cup \{p \in 2\mathbb{Z}+1\} \\
\Gamma(2): &\quad \{0,\ 1,\ \infty\} = \mathbb{Q}_{0/1} \cup \mathbb{Q}_{1/1} \cup \mathbb{Q}_{1/0}.
\end{aligned} \tag{12}$$

Finally, for completeness it should be mentioned that there are other discontinuous groups, not contained in $\Gamma(1)$, acting on the upper half plane. However, the geometrical notions developed for $\Gamma \subseteq \Gamma(1)$ can readily be generalized to such groups. Since $\mathbb{H} \cong \mathrm{SL}(2,\mathbb{R})/\mathrm{SO}(2)$, every discontinuous group Γ of analytic automorphisms on $\mathbb{H}$ is a subgroup of $\mathrm{SL}(2,\mathbb{R})$, i.e. any $\gamma \in \Gamma$ is realized as a real fractional transformation of the upper half plane which leaves the real line invariant. The data determining Γ are precisely those of physical interest: the set of limit points $\mathbb{L}$ on the real line, and the shape of the fundamental domain $\mathbb{F}_\Gamma$. Because the hyperbolic metric on $\mathbb{H}$ is $\mathrm{SL}(2,\mathbb{R})$ invariant, $\mathbb{F}_\Gamma$ can always be constructed as a polygon bounded by geodesics of this metric. Provided $\mathbb{F}_\Gamma$ has a finite number of sides, which seems physically reasonable since otherwise the phase boundaries would be pathological indeed, Γ is finitely generated and $\mathbb{L}$ is infinite. Such groups are called Fuchsian. If $\mathbb{L}$ is the entire real line, thus providing an impenetrable barrier against analytical continuation into the lower half plane, the group is said to be "Fuchsian of the first kind", and the modular group is of this type.

4 Phase and Flow Diagrams

Before considering physical applications in the next section, we first complete a taxonomy of the phase and flow diagrams associated with the generalized KW-symmetries introduced above. This is most easily done by invoking the discussion of C-functions from Sect. 2.

It is clear that the C-function must be a real valued function automorphic under $\Gamma \subset \Gamma(1)$, but we are not able to identify the exact form of this function since that would amount to a complete solution of the non-perturbative problem. So while the detailed form of the C-function will vary from system to system (and also with the choice of action and parametrization representing the system, but this will not change the universality class), thus allowing the critical exponents and other universal quantities to change, the general structure of the phase diagram will not, and that constrains the possible flow patterns severely.

Consider first the simplest example, which is the full modular group. The phase diagram, as well as one of the few flow patterns consistent with this phase structure, was already discussed above (Fig. 2). Any "C-function" automorphic under $\Gamma(1)$ will give rise to this phase diagram, and the simplest such function is $|J|^2 = J\bar{J}$, where $J(z)$ is Klein's famous absolute invariant of $\Gamma(1)$.

The easiest way to plot this function is to use the fact that every automorphic function at level two is a rational function of the absolute invariant (λ) of $\Gamma(2)$. Since $\Gamma(2)$ is a (normal) subgroup of $\Gamma(1)$, J must also be a rational function of λ:

$$J = \frac{4}{27}\frac{(\lambda^2 - \lambda + 1)^3}{\lambda^2(\lambda - 1)^2}. \tag{13}$$

The virtue of this representation is that

$$\lambda = \frac{\vartheta_2^4}{\vartheta_3^4}, \tag{14}$$

and the power-series expansions in $q = \exp(\pi i z)$ of the theta-functions are rapidly converging *simple* sums:

$$\vartheta_2(z) = \sum_{n=-\infty}^{\infty} q^{(n+\frac{1}{2})^2}, \quad \vartheta_3(z) = \sum_{n=-\infty}^{\infty} q^{n^2}, \quad \vartheta_4(z) = \sum_{n=-\infty}^{\infty} (-)^{n^2} q^{n^2}. \tag{15}$$

(ϑ_4 is included for future reference.)

Because $|J|$ has zeros, at all elliptic fixed points of order three, this function cannot be a physical C-function, which must be bounded from above and below (cusp form). This is easily remedied by considering slightly more general rational functions of $|J|$, and does not affect the topology of the phase diagram. As a more "realistic" illustration consider a bounded function exhibiting flow towards the

parabolic fixed points on the real axis, e.g. $C_J \equiv (1+|J|)^{-1}$. Fig. 3 shows a plot of C_J which was evaluated using only the first few terms in the theta-expansions given above. The bizarre behaviour along the real line, as $\mathrm{Im}\, z \to 0$, is necessary because the landscape keeps undulating arbitrarily close to the real line.

The phase and flow diagram (Fig. 2) is now easily extracted. The flow lines and phase boundaries are orthogonal to the contour (equipotential) levels $C_J = \text{const}$. Since $J(z)$ is a holomorphic function it is also conformal, so it preserves angles. The flow lines are therefore the contour lines of $\arg(J)$, some of which are plotted in Fig. 2. The displayed flow lines are the shortest paths (i.e. geodesics) between any two fixed points, in the natural (hyperbolic or Poincaré) metric on the upper half plane. All geodesics in this metric are circles orthogonal to the real axis, possibly of infinite radius, i.e. vertical lines.

Another flow pattern consistent with $\Gamma(1)$ is obtained by interchanging attractive and repulsive points, which gives the flow generated by J itself. If we insist that all the attractors be parabolic, i.e. $\oplus = \mathbb{P}$, there are still two more possibilities. The tree can be marginal (i.e. no flow on the tree), which corresponds to two coupled Ising models (= Baxter model) in the coupled clock model ($p = 2$). Or we could reverse the directions of the flow on the tree, in which case $\mathbb{E}_2$ points are repulsive and $\mathbb{E}_3$ points are (three-way) monkey saddles, corresponding to coupled clock models with $p > 2$, e.g. coupled 3-state Potts models. The latter example shows that we are not restricted to consider only ordinary (two-way) saddle points, a fact which will be important below when we construct flow diagrams for $\Gamma(2)$. In anticipation of that discussion, let us introduce $\circledast_n$ to denote a monkey saddle of order n (a saddle for a monkey with $n-2$ tails), i.e. a mountain pass surrounded by n peaks and n valleys. Obviously $\circledast_2 = \otimes$.

In short, we have in a somewhat heuristic but rather transparent way recovered the same result as we obtained in Sect. 3 by a more formal argument. A great virtue of this approach is that we now immediately can repeat the analysis for congruence subgroups of $\Gamma(1)$. The only result we need about their modular forms is that the absolute automorphic functions (i.e. modular forms of weight zero) of $\Gamma_{\mathrm{T}}(2)$, $\Gamma_{\mathrm{S}}(2)$ and $\Gamma_{\mathrm{W}}(2)$ are:

$$f_T = (\lambda - 1)\lambda^{-2}, \quad f_S = \lambda(1-\lambda), \quad f_W = -\lambda(1-\lambda)^{-2}. \tag{16}$$

Note also that the more familiar theta-functions ϑ_2, ϑ_3 and ϑ_4 appear naturally in this context as entire modular forms of weight 1/2 for the groups $\Gamma_{\mathrm{T}}(2)$, $\Gamma_{\mathrm{S}}(2)$ and $\Gamma_{\mathrm{W}}(2)$, respectively.

As already explained in Sect. 3 the unique subgroup which respects the parity of the denominator of the parabolic fixed points appearing at the rational numbers (p/q) on the real line, is $\Gamma_{\mathrm{T}}(2)$. The phase and flow diagram associated with this symmetry is determined by the "C-function" $C_T \equiv |f_T|$ or its inverse, depending on which subclass ($\{q \text{ odd}\}$ or $\{q \text{ even}\}$) of parabolic fixed points we wish to be attractors ($\oplus$). A plot of C_T is shown in Fig. 4, from which it is immediately evident that only "odd" phases can appear. The corresponding phase and flow diagram is shown in Fig. 5.

There is another phase and flow diagram associated with $\Gamma_{\mathrm{T}}(2)$, where only "even" phases appear as stable fixed points. This "dual" flow pattern is generated by the "C-function" C_T^{-1}, which is plotted in Fig. 6. The corresponding phase and flow diagram, which can also be obtained from Fig. 5 by interchanging the attractive and repulsive fixed points, reversing the arrows on all flow lines, and interchanging the flow lines and phase boundaries passing through saddle points, is shown in Fig. 7.

Fortunately, aside from $\Gamma(2)$ itself, we have now found all phase diagrams that appear at level two, up to translation and rescaling, as we now explain. Since the space of automorphic functions (weight=0) of $\Gamma \subset \Gamma(1)$ is one-dimensional, it is sufficient to discuss the connection between the "prototype C-functions" $C_R^2 \equiv f_R \bar{f}_R$ $(R = T, S, W)$. The reason that these are not independent is that the congruence groups are conjugate to each other:

$$\Gamma_{\mathrm{S}}(2) = P^{-1}\Gamma_{\mathrm{T}}(2)P, \quad \Gamma_{\mathrm{W}}(2) = S^{-1}\Gamma_{\mathrm{T}}(2)S. \tag{17}$$

This can be seen by conjugating the generators of one group and using the fundamental identities $S^2 = P^3 = 1$ to show that this gives the generators of the conjugate group. Now let f and $\tilde{f}$ denote functions automorphic under Γ and $\tilde{\Gamma}$, respectively, i.e. $f(G(z)) = f(z)$ for all $G \in \Gamma$ and $\tilde{f}(\tilde{G}(z)) = \tilde{f}(z)$ for all $\tilde{G} \in \tilde{\Gamma}$. If $\tilde{\Gamma} = L^{-1}\Gamma L$ with $L \in \Gamma(1)$, then $f(L(z)) = \tilde{f}(z)$. This follows from $f(L(z)) = f(GL(z)) = f(LL^{-1}GL(z)) = f(L(\tilde{G}(z)))$, where $\tilde{G} = L^{-1}GL \in \tilde{\Gamma}$, which states

that $f(L)$ is automorphic under $\tilde{\Gamma}$. For example, because $\Gamma_W(2) = S\Gamma_T(2)S$, we now immediately know that $f_T(S) \sim f_W$. The exact relation can be derived from the transformation properties of λ [14]:

$$\begin{aligned} &\lambda(T) = (\lambda - 1)^{-1}, \quad \lambda(S) = (1 - \lambda), \quad \lambda(W) = \lambda^{-1} \\ &\lambda(P) = (1 - \lambda)^{-1}, \quad \lambda(P^2) = 1 - \lambda^{-1} \end{aligned} \tag{18}$$

from which it follows that

$$\begin{aligned} f_T(T) = f_W(S) &= f_S(W) = f_W(P) = f_S(P^2) \\ f_S(T) = f_T(S) &= f_W(W) = f_S(P) = f_T(P^2) \\ f_W(T) = f_S(S) &= f_T(W) = f_T(P) = f_W(P^2). \end{aligned} \tag{19}$$

Finally, we also need the doubling formulas for theta-functions

$$\begin{aligned} &2\vartheta_2^2(2z) = \vartheta_3^2(z) - \vartheta_4^2(z), \quad 2\vartheta_2(2z)\vartheta_3(2z) = \vartheta_2^2(z) \\ &2\vartheta_3^2(2z) = \vartheta_3^2(z) + \vartheta_4^2(z), \qquad \vartheta_4^2(2z) = \vartheta_3(z)\vartheta_4(z) \end{aligned} \tag{20}$$

and the identity $\vartheta_4^4 = \vartheta_3^4 - \vartheta_2^4$. It is now straight-forward algebra to show that:

$$f_T^{-1}(z) = 16 f_S(2z + 1) = 16 f_W(2z). \tag{21}$$

Hence C_S and C_W are related to C_T^{-1} by rescaling (by a factor of two) followed by a translation, as asserted.

Finally we turn to the *pièce de résistance* at level two, which is the phase and flow diagram of $\Gamma(2)$ itself. It is generated by $C_\lambda \equiv |\lambda|^{-1}$, a plot of which is shown in Fig. 8.

Only parabolic fixed points now survive, which $\Gamma(2)$ partitions into three equivalence classes of type 0, 1 and ∞. The C-function must maintain this distinction, by assigning different types of fixed points to the three different classes. From Fig. 8 we see that C_λ solves this problem by having fixed points of type 0 be monkey saddles of infinite order: $0 = 0/1 = \circledast_\infty$, while $1 = 1/1 = \oplus$ and $\infty = 1/0 = \ominus$. In other words, at each parabolic point of type 0 there are an infinite number of attractive directions intertwined with an infinite number of repulsive directions. It is hard to imagine how this can happen without the function being very flat near the fixed point, which we see is indeed the case for $C_\lambda(\circledast)$.

Part of the resulting phase and flow diagram is shown in Fig. 9, which also contains both contour levels and non-geodesic flow lines, i.e. a complete representation of the complex function λ^{-1}.

5 Two-Dimensional Charge Transport

We are now finally ready to turn to the main application of these ideas, "anomalous" charge transport in effectively two-dimensional systems, specifically the quantum Hall system, which originally motivated the general discussion reviewed above, and high-temperature superconductivity.

In Ref. [1] it was suggested that the parameter space of conductivities of the quantum Hall system is invariant under the full modular group, and it was shown that this is consistent with all existing scaling experiments. The algebraic argument given there, leading to the phase and flow diagram shown in Fig. 2, can now be supplemented by the geometric analysis using C-functions given above. From the discussion in the previous section it should be clear that if the conductivity space parametrizing the low-energy effective theory describing the quantum Hall system is $\Gamma(1)$-invariant, then the true (physical) C-function (C_{QHS}) generating the RG-flow must be of the same mathematical genus as the function C_J shown in Fig. 3. The complex upper half plane is now parametrized by the complexified conductivity $\sigma \equiv \sigma_{xy} + i\sigma_{xx}$, or, equivalently, by the complexified resistivity $\rho \equiv \rho_{xy} + i\rho_{xx}$. Since $\rho = S(\sigma) = -1/\sigma$ (the resistivity tensor ρ_{ij} is by definition the inverse of the conductivity tensor σ_{ij}), and S is in $\Gamma(1)$, the phase and flow diagram looks exactly the same in resistivity space.

A rigorous derivation of the exact global form of C_{QHS} would amount to a complete non-perturbative solution of the quantum Hall problem, since then all universal (material independent) properties would be known, including the location of all fixed points, the observed "super-universality" of delocalization fixed points, and the values of the scaling exponents. It was shown in Ref. [1] that the first two follow from the existence of a generalized KW-symmetry alone, while the calculation of critical exponents, i.e. the curvature of C_{QHS} at fixed points, requires more detailed dynamical information [6]. A derivation of this type, from

the microscopic physics of electrodynamics in disordered two-dimensional media, via a mesoscopic "semi-effective" theory encoding the localization of anyons using the Chern-Simons trick, to a truly "effective" or macroscopic model whose space of transport coefficients exhibits KW-duality, could, at least from a field theoretical point of view, be said to constitute a complete solution of the quantum Hall problem. Our efforts in this direction will be described elsewhere [6].

We now explore the consequences of making a slightly weaker ansatz [7]. One of the motivations for this is that the phase and flow diagram invariant under the full modular group shown in Fig. 2 contains both "even" and "odd" phases, while the experiments *predominantly* turn up only "odd" phases. A phase is uniquely characterized by the value of the conductivity at the attractive fixed point to which it is attached (i.e., for which it is the basin of attraction or universality class): $\sigma_\oplus = \sigma_{xy} = p/q \in \mathbb{Q}$. If the denominator q is odd (even) a conductivity phase is called odd (even). Since experiments are turning up even fractions at an increasing rate it is certainly good not to have them disallowed by the family of infinite discrete symmetries that we are considering. On the other hand, it would be nice to be able to "switch them off", e.g. in a very strong magnetic field (B), since in this case the electron spins are completely polarized so that the spin degree of freedom is frozen out. This means that the spatial part of the many-body wave-function must be completely anti-symmetric, and consequently, by a standard argument due to Laughlin [15], only odd phases can appear in such a system. It is clear from a glance at (12) that this is exactly what happens if the $B \to \infty$ limit breaks $\Gamma(1)$-symmetry acting on the *conductivity space* to the subgroup $\Gamma_{\mathrm{T}}(2)$, since this is the only one that preserves the parity of the *denominator* q. If we instead consider resistivities, whose fixed point values are the inverse of $\sigma_\oplus$, $\rho_\oplus \equiv S(\sigma_\oplus) = -q/p$, the relevant subgroup is $\Gamma_{\mathrm{W}}(2)$, which preserves the parity of numerators. This is just a special case of (17), which states that these groups are related through conjugation by S.

Notice that $\Gamma_{\mathrm{T}}(2)$ is the group implicitly assumed in the so-called "hierarchy generating mechanism" [15, 16, 17], which was invented in order to account for the observed fractions (see also Ref. [18]). To see this recall that if a ground state with "filling factor" ν appears, then the particle-hole conjugate state with filling

factor $1-\nu$, as well as the quasi-particle condensate with filling factor $\nu/(2\nu+1)$ should also be ground states of the quantum Hall system. Since ν is essentially the Hall conductivity on the plateaus, we see that these are fractional linear transformations on σ restricted to act only on the real axis. The first transformation is $TJ = JT$, where $J : \sigma \to -\bar{\sigma}$ is a so-called "outer automorphism" of $\Gamma(1)$. J is in fact the only automorphism of $\Gamma(1)$ not in $\Gamma(1)$, and since J is rather trivial we will continue to suppress it here. The other transformation is the inverse of ST^2S, which together with T generates $\Gamma_{\mathrm{T}}(2)$, according to (11).

The $\Gamma_{\mathrm{T}}(2)$-invariant phase and flow diagram admitting only odd conductivity phases is the shown in Fig. 5. From (21) it follows that the $\Gamma_{\mathrm{W}}(2)$-invariant resistivity diagram is given by C_T^{-1}, whose phase and flow diagram is shown in Fig. 7, rescaled by a factor of two. These two diagrams contain exactly the same physical information about the quantum Hall system, plotted in different but equivalent "coordinates". And as in the case of the full modular group [1], they contain an infinite number of robust predictions which can be checked by performing scaling experiments. They are not yet precise enough to distinguish between these symmetries, but appear at the moment to favour the full modular group [7]. More experiments of this type would be highly desirable.

In the mean time we should pursue this group-theoretical line of reasoning, and ask if the other congruence groups also encode properties of two-dimensional charge transport. These groups generate distinct, but closely related, conductivity hierarchies that may be of interest for "relatives" of the quantum Hall system [19], including the frustrated Heisenberg antiferromagnet and high-temperature superconductivity, where the "fundamental" charge carriers are bosons rather than fermions.

It has been argued that materials exhibiting high-temperature superconductivity may be related to states with even filling factors. This idea is based on a chain of conjectures linking Anderson's spin-liquid ("resonating valence bond (RVB)") states [20] to Laughlin's fractional quantum Hall states (which describe the system when it is at the attractive fixed points) [15].

The RVB quantum spin-liquid was originally invoked as a ground state of the frustrated Heisenberg antiferromagnet, but more recently Anderson has ar-

gued that it is essential for understanding high-temperature superconductivity [21]. On the other hand, following up on an observation by Lee and Joannopoulos, Kalmeyer and Laughlin [22] concluded that this state is essentially the same as a fractional quantum Hall state for bosons. Subsequently, Laughlin [19] argued eloquently that quantum Hall states provide the "canonical paradigm" for spin-liquids in general, and high T_c in particular. In other words, he argues that the physics of a fractional quantum Hall state does not depend crucially on the presence of a real magnetic field; it is a condensed state to be expected in many situations, perhaps whenever fractional quantum numbers and anomalous statistics is possible.

If this is all true, then it is natural to conjecture, by analogy with the real quantum Hall system, that there may be a hierarchy of superconducting states in these effectively two-dimensional materials [23, 24]. If the hierarchy generating mechanism is the same as in the quantum Hall system we expect the relevant group to be $\Gamma_{\mathrm{T}}(2)$. Since it relates all even fractions, starting from the bosonic Laughlin state with filling factor 1/2 we can generate all the even states [25], and the corresponding $\Gamma_{\mathrm{T}}(2)$-invariant phase and flow diagram is the one shown in Fig. 7.

However, because there appears to be some confusion as to exactly what constitutes "a bosonic hierarchy", there is an interesting alternative suggested by Lee and Fisher [24]. Using a kind of duality argument applied to a gas of anyons they find a hierarchy of Laughlinesque states with statistics parameter

$$\nu = \langle a_0, a_1, \ldots, a_n \rangle \equiv \frac{1}{a_0 + \frac{1}{a_1 + \ldots + \frac{1}{a_n}}} \equiv \frac{p}{q}, \tag{22}$$

where the a_i $(i = 0, 1, \ldots, n)$ are even integers. This represents a state in which q anyons (quasiparticles in the fractional quantum Hall effect) bind to become bosons that condense into a charge $Q = qe$ superfluid with flux quantum hc/Q. They also claim that (22) is the same as the hierarchy for the filling factor in the boson fractional quantum Hall effect.

Both even and odd q appear in this bosonic hierarchy of anyon superconducting states, but p/q is either of type $0/1 = 0$ or of type $1/0 = \infty$. This follows from the continued-fraction expansion of a rational number [26]. Every fraction

satisfies $p/q = \langle a_1, a_2, \ldots, a_n \rangle$, with a_i positive or negative even integers, with the possible exception of a_n which may be odd. Each rational of type 0 has a unique expansion $p/q = \langle a_0, \ldots, a_{2m+1} \rangle$ with a_{2m+1} even. Similarly, each rational of type ∞ has a unique expansion $p/q = \langle a_0, \ldots, a_{2m} \rangle$ with a_{2m} even. But for rationals of type 1 the last partial quotient is odd and this leads to infinitely many expansions $\langle a_1, \ldots, a_n \rangle = \langle a_1, \ldots, a_n + 1, 2, 2, \ldots, 2, 1 \rangle$. We see that the hierarchy in (22) appears to consist only of type 0 and type ∞ states, i.e. fractions with pq even. A glance at (12) reveals that the group partitioning $\mathbb{Q}$ into two equivalence classes defined by $pq \in 2\mathbb{Z}$ and $pq \in 2\mathbb{Z} + 1$ is *not* $\Gamma_{\mathrm{T}}(2)$, but rather $\Gamma_{\mathrm{S}}(2)$.

Note also that unlike the conventional superconducting situation, because the anyon gas is not time-reversal invariant a Hall conductivity can and *does* appear [24]. It may therefore be of experimental interest to consider the phase and flow diagrams associated with $\Gamma_{\mathrm{S}}(2)$. It follows from (21) that this is the diagram in Fig. 7, rescaled by a factor of two and then shifted by one to the right.

6 Concluding Remarks

The question now arises whether it is possible to reconcile the two phase and flow diagrams discussed here for the quantum Hall system, or if they are mutually exclusive. Ideally, we would, perhaps, like Fig. 5 to emerge from Fig. 2 in the strong magnetic field limit. At an algebraic or group-theoretical level it is not too difficult to imagine symmetry breaking terms in the action which, when switched on, break the parameter space symmetry down to some subgroup representing the surviving symmetries. But how is this reflected in the structure of the phase and flow diagram? With the physical and geometrical picture of RG-potentials described above in mind, it seems natural to conjecture that there exists an "interpolating C-function" for electron transport in two dimensions, which is a linear combination of pieces automorphic under the various subgroups respected by symmetry breaking perturbations. For example, for the quantum Hall system we would write $C = f(B)C_{\mathrm{odd}} + g(B)C_{\mathrm{even}}$, where the coefficient functions f and g may depend on external parameters such as temperature and disorder in addition to the parity breaking external magnetic field B. Provided that

$f(B \to \infty) \to 0$, we can with this scheme turn all even (or odd) fractions off at will, simultaneously and continuously. It is not clear whether this can be done without also continuously changing the critical exponents, but it seems to be an interesting question worth answering.

Let us conclude with a philosophical remark. Following Laughlin and others, we have argued above that the complicated hierarchical phase structure discussed here is not restricted just to the *bona fide* quantum Hall situation. Frustrated Heisenberg antiferromagnets and high-temperature superconductors may perhaps provide other examples. If this is true it would be useful to develop some kind of intuition for when this kind of behaviour is to be expected. What these systems seem to have in common is *frustration*, in the quantum Hall case caused by a competition between Bose condensation and Fermi exclusion. In two dimensions, where anomalous statistics is possible, such competition may force the system to compromise on a ground state whose excitations are anyonic, i.e. intermediate between the two extremes to which we are restricted in higher dimensions. These quasi-particles may again condense, when conditions are favourable, into yet another compromise, etc., and the complicated cooperative behaviour encoded in the hierarchical phase and flow diagrams emerges. The infinite non-abelian discrete symmetries discussed here formalize this idea. If this philosophy is useful, then such behaviour should be manifest in other frustrated low-dimensional systems as well. Indeed, examples are not hard to find: the phase diagram of the ANNNI model (see Ref. [27] for a review), the prototype for systems exhibiting commensurate-incommensurate phase transitions, bears a striking resemblance to Fig. 2.

Acknowledgments

It is a pleasure to thank P. Aspinwall, P. Candelas, J. Latorre, F. Quevedo, G. Ross, C. Series and T. Skjelbred for useful discussions. This work was supported by the Norwegian Research Council for Science and Humanities (NAVF) and the British Science and Engineering Research Council (SERC).

References

[1] C.A. Lütken and G.G. Ross, Phys. Rev. **B45** (1992) 11837

[2] J.L. Cardy and E. Rabinovici, Nucl. Phys. **B205** (1982) 1

[3] J.L. Cardy, Nucl. Phys. **B205** (1982) 17

[4] S.M. Girvin and A.H. MacDonald, Phys. Rev. Lett. **58** (1987) 1252

[5] J.M. Leinaas and J. Myrheim, Il Nuovo Cimento **37** (1977) 1

[6] C.A. Lütken and G.G. Ross, *Delocalization, Duality and Scaling in the Quantum Hall System*, in preparation

[7] C.A. Lütken, *Global Phase Diagrams for Charge Transport in Two Dimensions*, Oxford University preprint OUTP-9216P (July 1992)

[8] H.A. Kramers and G.H. Wannier, Phys. Rev. **60** (1941) 252

[9] D.J. Wallace and R.K.P. Zia, Ann. Phys. (NY) **163** (1975) 142

[10] A.B. Zamolodchikov, JETP Lett. **43** (1986) 730; Sov. J. Nucl. Phys. **46** (1987) 1090

[11] D. Friedan, lecture at the Nordisk Forskarkurs, Recent developments in quantum field theory, July 1990, Laugarvatn, Iceland, unpublished; A. Cappelli, D. Friedan and J.I. Latorre, Nucl. Phys. **B352** (1991) 616

[12] J. Cardy, *in* Fields, strings and critical phenomena, Les Houches summer school 1988, eds. E. Brézin and J. Zinn-Justin (North-Holland, Amsterdam, 1990)

[13] R.J. Baxter, Phys. Rev. Lett. **26** (1971) 832

[14] R.A. Rankin, Modular Forms and Functions (Cambridge University Press, Cambridge, 1977)

[15] R. Laughlin, Phys. Rev. Lett. **50** (1983) 1395

[16] F.D.M. Haldane, Phys. Rev. Lett. **51** (1983) 605

[17] B. Halperin, Phys. Rev. Lett. **52** (1984) 1583

[18] A.H. MacDonald, G.C. Aers and N.W.C. Dharma-wardana, Phys. Rev. **B31** (1985) 5529

[19] R.B. Laughlin, Science **242** (1988) 525

[20] P.W. Anderson, Mater. Res. Bull. **8** (1973) 153

[21] P.W. Anderson, Science **235** (1987) 1196

[22] V. Kalmeyer and R.B. Laughlin, Phys. Rev. Lett. **59** (1987) 2095

[23] X.-G. Wen, F. Wilczek and A. Zee, Phys. Rev. **B39** (1989) 11413

[24] D.-H. Lee and M.P.A. Fisher, Phys. Rev. Lett. **64** (1990) 1313

[25] S-J. Rey and A. Zee, Nucl. Phys. **B352** (1991) 897

[26] R. Moeckel, Ergod. Th. & Dynam. Sys. **2** (1982) 69

[27] W. Selke, Phys. Rep. **170** (1988) 213

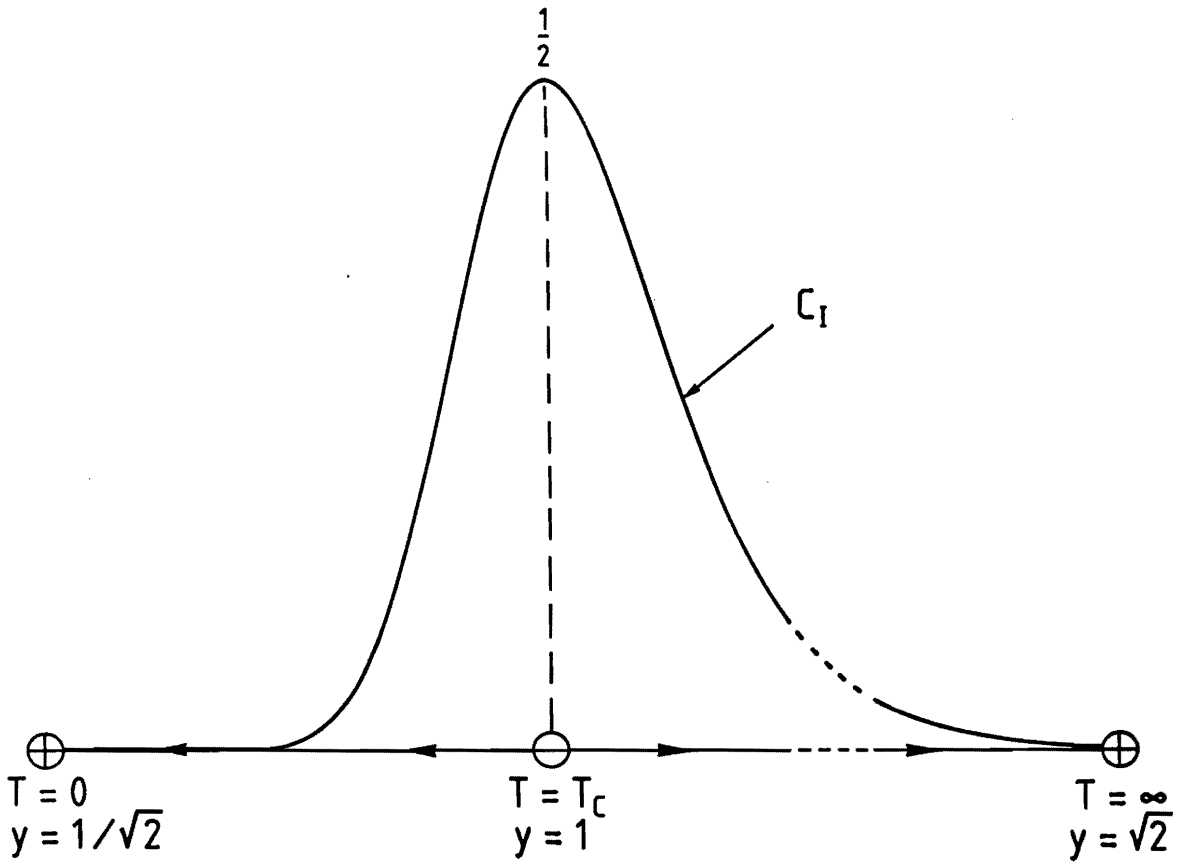

Figure 1: Phase and flow diagram of the two-dimensional Ising model, "projected down" from a C-function whose gradient generates the flow.

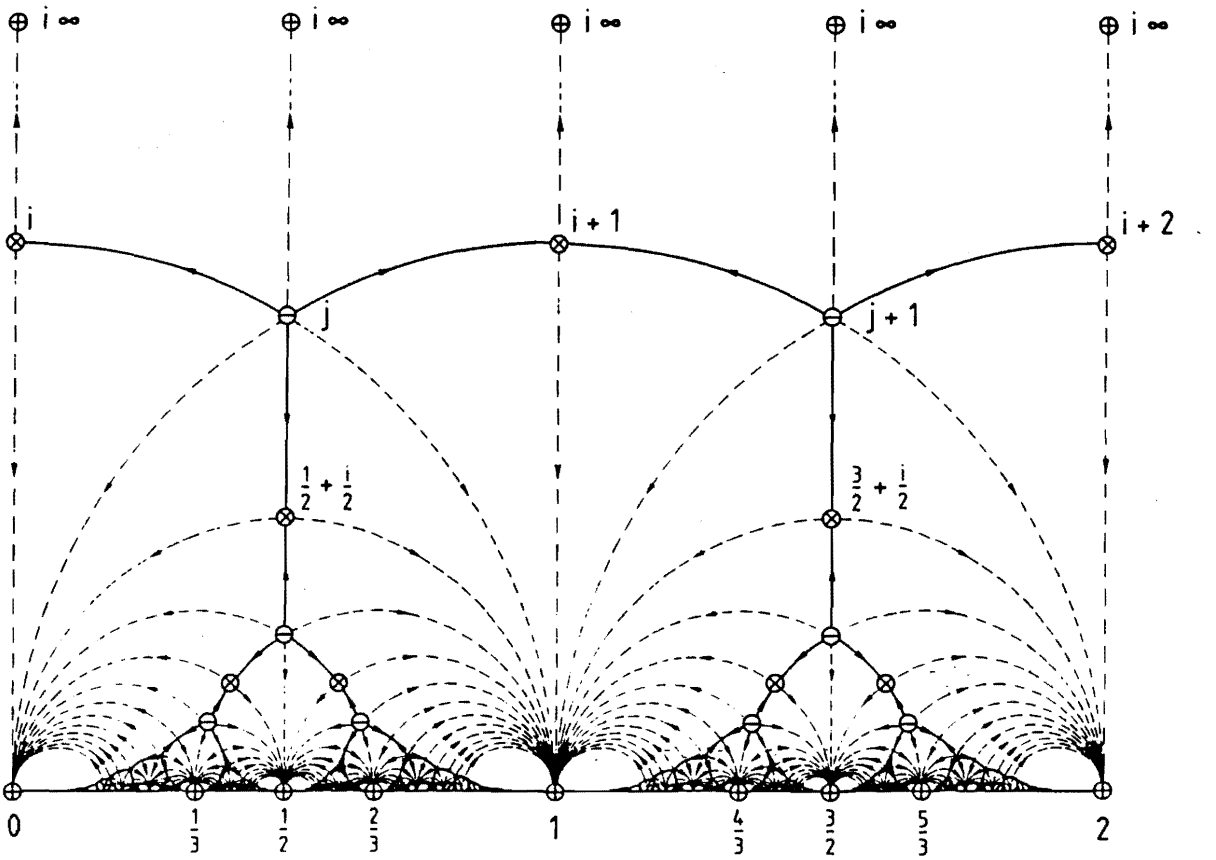

Figure 2: Phase and flow diagram determined by $\Gamma(1)$, showing both "odd" and "even" phases.

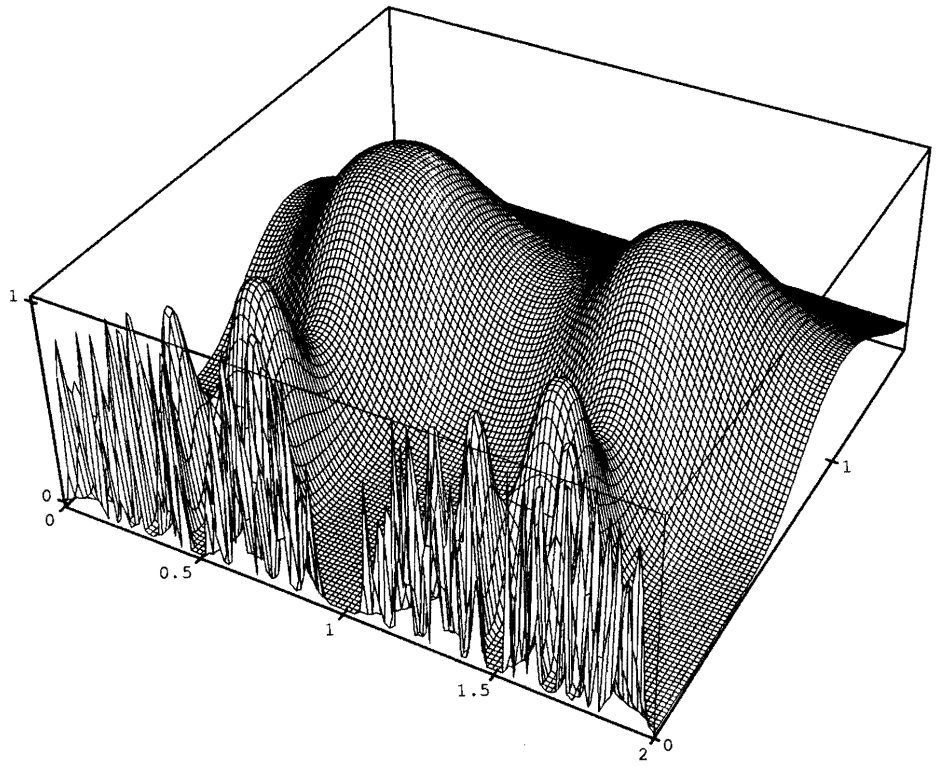

Figure 3: $\Gamma(1)$-invariant "C-function" C_J, which gives the phase and flow diagram in Fig. 2.

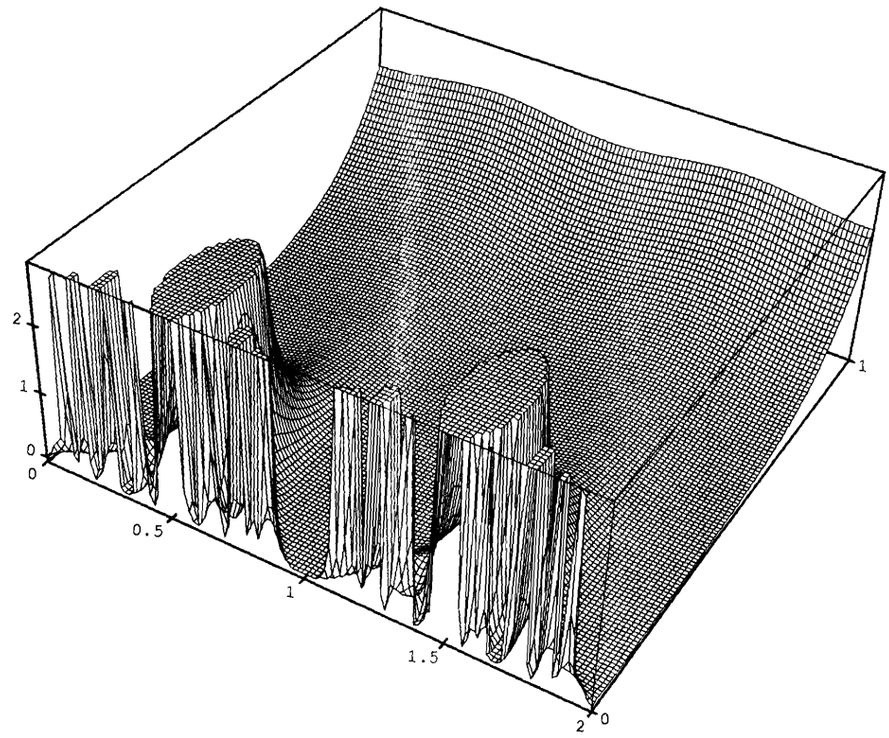

Figure 4: $\Gamma_T(2)$ invariant "C-function" C_T.

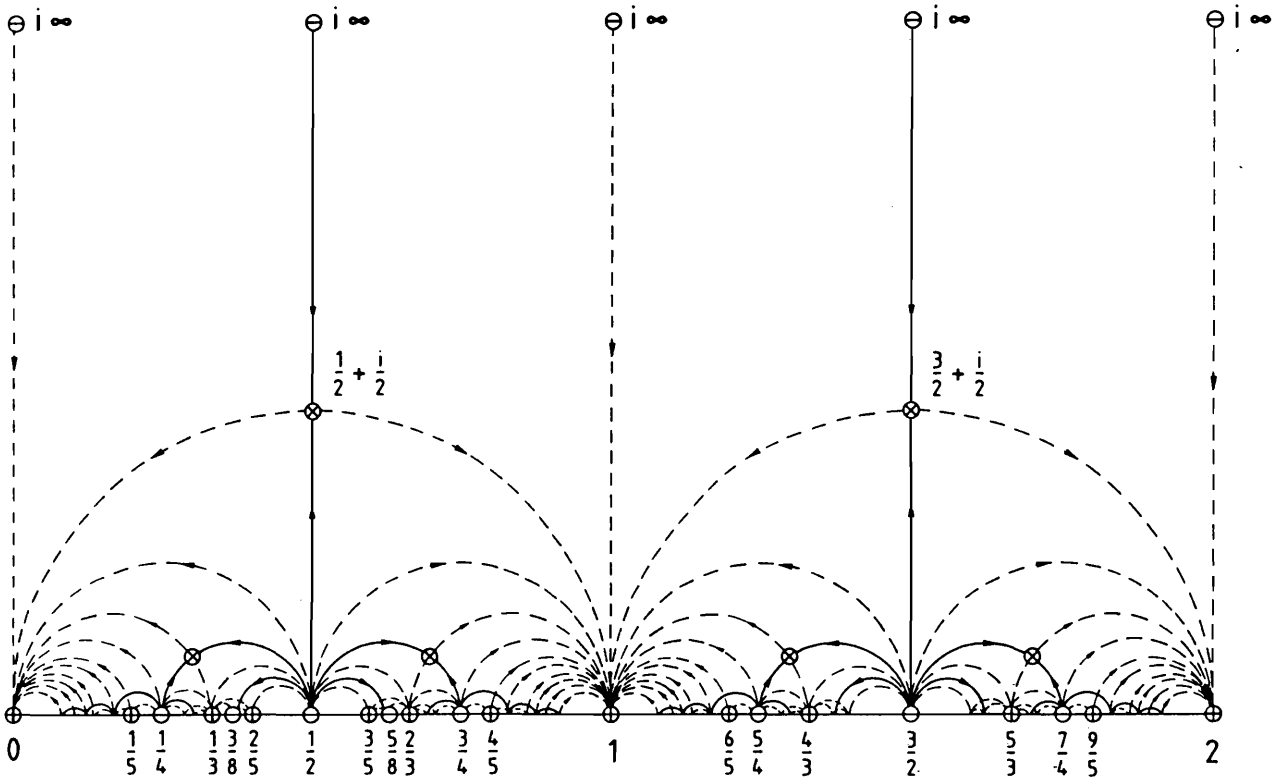

Figure 5: Phase and flow diagram of the "C-function" C_T displayed above, showing only "odd" phases.

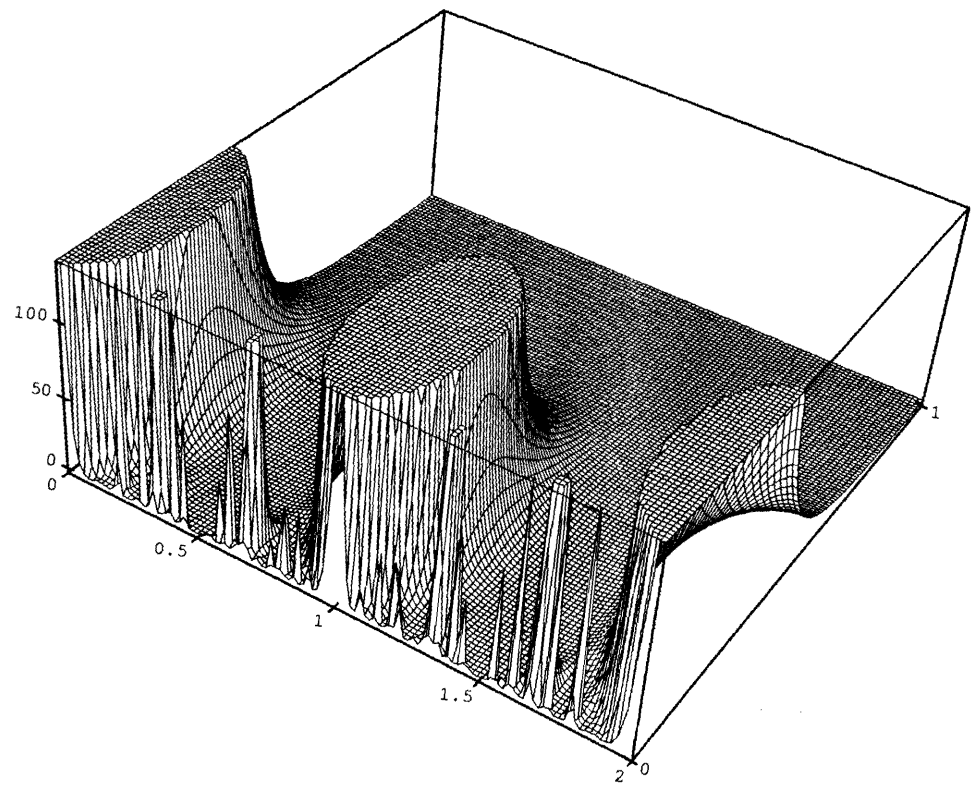

Figure 6: $\Gamma_T(2)$ invariant "C-function" C_T^{-1}.

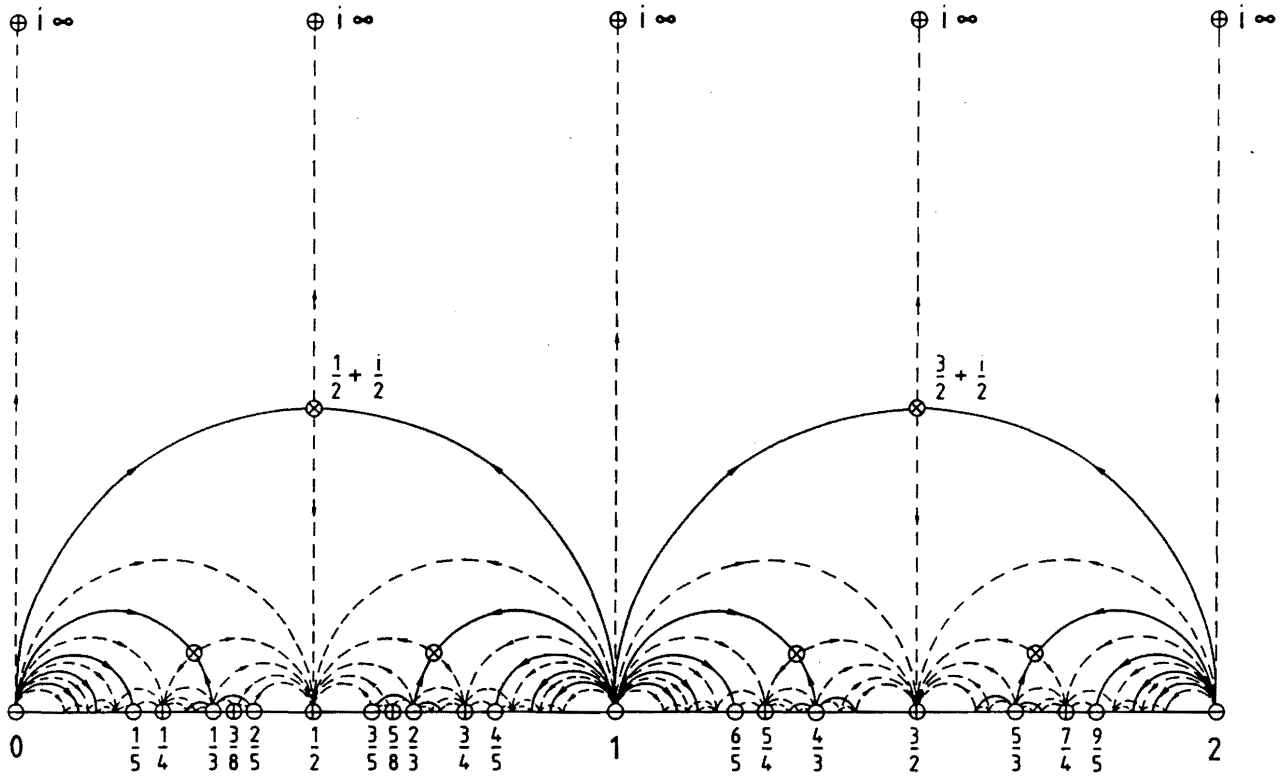

Figure 7: Phase and flow diagram of the "C-function" C_T^{-1}, showing only "even" phases.

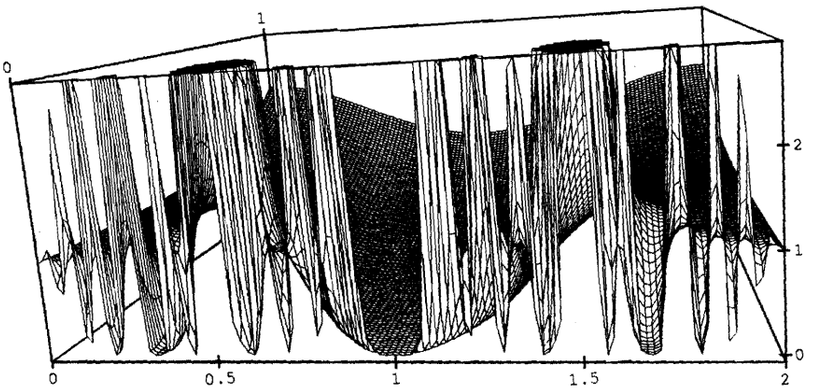

Figure 8: $\Gamma(2)$ invariant "C-function" C_λ.

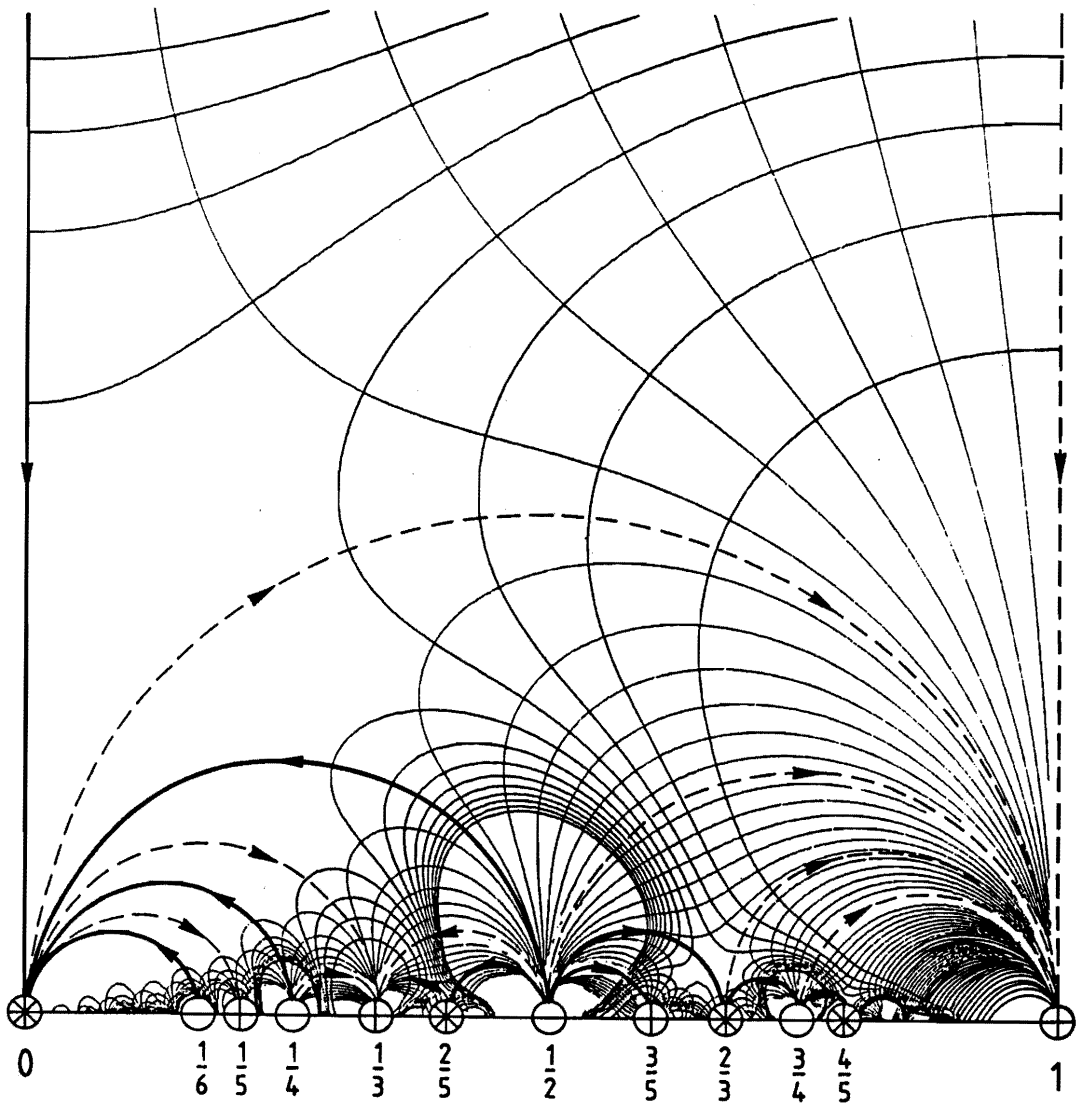

Figure 9: Phase and flow diagram of the "C-function" C_λ, showing only phases of type 1. Thick lines are phase boundaries, thin lines are contour levels of constant $\mathrm{abs}(C_\lambda)$ and constant $\arg(C_\lambda)$ (flow lines), and broken lines are geodesic flow lines (in the hyperbolic metric on $\mathbb{H}$).